Proceedings of ASME Turbo Expo 2011
GT2011
June 6-10, 2011, Vancouver, British Columbia, Canada

GT2011-45453

INVESTIGATION OF CORIOLIS EFFECT ON VIBRATION CHARACTERISTICS OF A REALISTIC MISTUNED BLADED DISK

Jianqiang Xin
School of Jet Propulsion
Beijing University of Aeronautics and Astronautics
100191 Beijing, China
Email: xjq@sjp.buaa.edu.cn

Jianjun Wang*
School of Jet Propulsion
Beijing University of Aeronautics and Astronautics
100191 Beijing, China
Email: wangjianjun@buaa.edu.cn

ABSTRACT

Mistuning, which refers to inevitable variations in blades properties, will change the vibration of bladed disks dramatically. Bladed disks are exposed to effects of forces caused by bladed disk rotation, such as centrifugal and Coriolis forces. However, there is little research on the vibration behavior of a realistic bladed disk with Coriolis force. An investigation of the speed effect, i.e., the effects of centrifugal and Coriolis forces, on the vibration characteristics of a realistic mistuned bladed disk model is presented in this paper. Finite element method (FEM) is used to obtain the system mass, stiffness and damping matrix. The effects of Coriolis force and centrifugal force on the modal frequency and harmonic response characteristics of tuned bladed disk are investigated first, then the modal localization and response characteristics of mistuned bladed disk are researched. This investigation indicates that: Coriolis force has efficient influences on the modal and response characteristics of a realistic mistuned bladed disk: it can both increase and decrease the localization of the mistuned bladed disk for different situations.

INTRODUCTION

Theoretically, bladed disks used in turbine engines are designed to be cyclically symmetry. However, due to the manufacturing process and material inhomogeneities, blade-to-blade variations in bladed disk occur and these variations are known as mistuning. Mistuning cause mode localization and vibration response amplification resulting in higher peak stresses than peak stresses predicted with a cyclically symmetric bladed disk model. The vibration characteristics of mistuned bladed disks have been widely studied for more than thirty years [1] [2] [3] [4] [5]. There are two surveys published by Wang [6] and Castanier [7] which present comprehensive and insightful literature information in this field.

The rotor of a high speed jet engine may be brought into vibration problems with rotating effect such as gyroscopic moment. Owing to the complexity of this problem, the majority of previous works have been confined to analysis of individual blade [8] [9], showing that Coriolis force has little impact on the vibration characteristic of the individual blade.A shaft- disk assembly is one of the most important components in turbomachinery such as gas turbines. The traditional approaches of rotordynamics were focused on the gyroscopic effect, which is a direct result of Coriolis force. However, the model of the classical rotordynamics was a rigid disc and a flexible shaft system, which could not consider the effect of the disk stiffness. Along with the design trend toward high performance and efficiency, analysis of rotors with assumed rigid disc could not predict the vibration characteristics in many cases. Thus, to get a better understanding and an accurate prediction of the dynamic characteristics of turbomachinery, some scholars began to model a flexible shaft, a flexible disk and a flexible blades system as an assembly, in which all the elements were dynamically coupled together [11] [12] [13] [14]. They found that the shaft mode can occur only with 0 and 1 nodal diameter mode shape of bladed-disk, and the frequencies of these coupling vibration modes are capable of splitting into backward and forward pair sets. But they

*Address all correspondence to this author.

did not consider mistuning effect, which is one of the key factors that impact the coupling of system modes. All of the above studies considered the influence of the stiffness of the bladed-disk on the dynamic characteristics of the system, but did not consider Coriolis effects on the vibration characteristics of the blade-disk itself.

However, Coriolis effects can generate significant changes in the dynamic properties for bladed disk, and especially for mistuned assemblies [15]. Two scholars [15] [16] investigated the vibration characteristics of the bladed-disk assembly with consideration of Coriolis effects recently, and both of them considered mistuning effect. Huang and Kuang [16] studied the vibration characteristics of a mistuned bladed-disk, and Nikolic et al. [15] performed vibration analysis of two types of models with considering Coriolis effects. However, both of them calculated with a theoretical model,which could not be applied to the engineering practice.

As the geometry of the bladed disk can influence the effect of Coriolis on the vibration characteristics significantly, it is necessary to use the realistic bladed disk for study. Thus, this paper is directed at investigating the speed effects, i.e., the effects of centrifugal and Coriolis forces, on the vibration characteristics of a realistic mistuned bladed disk model. The theory of bladed disk dynamics with rotating effect is derived in the second section and the finite element model of a realistic bladed disk is presented in the third section. Coriolis effect and centrifugal effect on the modal frequency characteristics of tuned bladed disk are investigated in the fourth section, and the frequency split phenomenon is studied in this section. In the fifth section, Coriolis Influence factor(CIF) is defined to calculate Coriolis effects on the mode localization phenomenon. In the sixth section, the backward and forward traveling wave responses of a tuned bladed disk are calculated. In the seventh section, the response characteristics of mistuned bladed disk with three kinds of mistuning patterns are studied to investigate Coriolis effects on the response amplitude of each blade. The conclusions from this study are summarized in the eighth section.

Theory

A bladed disk assembly model is shown in Fig.1, two frames are defined: $OXYZ$ is a stationary reference frame and $oxyz$ is a rotating reference frame fixed to the rotating undeformed bladed disk system. Origin o is assumed to coincide with the center of the disk. Point P is the undeformed position of a given material point of the structure while point P' represents the deformed position of this point. The position of point P with reference to the rotating reference ($oxyz$) is $\vec{r_0} = [x_0, y_0, z_0]^T$, while the position of P' with reference to ($oxyz$) is $\vec{r} = [x, y, z]^T$, and with reference to ($OXYZ$) is $\vec{R}$. Vector $\vec{\Omega} = \vec{a}\Omega$ is the rotational velocity of the rotating reference frame, and $\vec{a} = [a_x, a_y, a_z]^T$. The elastic displacement of point P as observed in the rotating frame

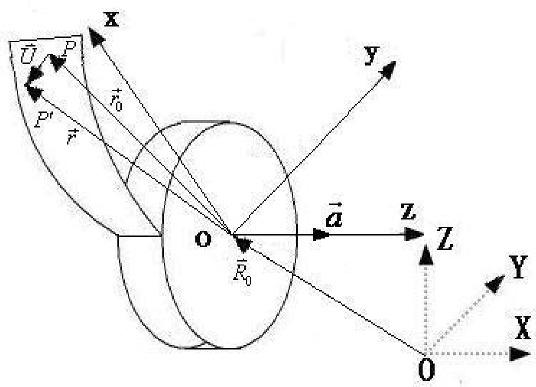

FIGURE 1: The bladed disk model

is defined as $\vec{U} = [u, v, w]^T$:

$$\vec{U} = \vec{r} - \vec{r_0} \tag{1}$$

and the velocity and the acceleration of point P as observed in the rotating reference frame:

$$\dot{\vec{r}} = \dot{\vec{r_0}} + \dot{\vec{U}} = \dot{\vec{U}} \tag{2}$$

and

$$\ddot{\vec{r}} = \ddot{\vec{U}} \tag{3}$$

Then, the velocity and acceleration of point P in the stationary reference frame is defined as:

$$\dot{\vec{R}} = \dot{\vec{U}} + \vec{\Omega} \times \vec{r} \tag{4}$$

and

$$\begin{aligned} \ddot{\vec{R}} &= \ddot{\vec{r}} + \vec{\Omega} \times (\vec{\Omega} \times \vec{r}) + 2\vec{\Omega} \times \dot{\vec{r}} \\ &= \ddot{\vec{U}} - \Omega^2 [S]^T [S] \vec{U} - \Omega^2 [S]^T [S] \vec{r_0} + 2\Omega [S] \dot{\vec{U}} \end{aligned} \tag{5}$$

where$[S]$ is

$$[S] = \begin{bmatrix} 0 & -a_z & a_y \\ a_z & 0 & -a_x \\ -a_y & a_x & 0 \end{bmatrix} \tag{6}$$

in which $\vec{\Omega}\times(\vec{\Omega}\times\vec{r})$ and $2\vec{\Omega}\times\vec{r}$ are centrifugal load term and Coriolis force term, respectively. Then the force acting on unit volume can be expressed as follows:

$$\begin{aligned}\vec{F}_g &= -\rho\vec{\ddot{R}}\\ &= -\rho\begin{bmatrix}\ddot{u}\\ \ddot{v}\\ \ddot{w}\end{bmatrix}+\rho\Omega^2[S]^T[S]\begin{bmatrix}u\\ v\\ w\end{bmatrix}\\ &\quad+\rho\Omega^2[S]^T[S]\begin{bmatrix}x_0\\ y_0\\ z_0\end{bmatrix}-2\rho\Omega[S]\begin{bmatrix}\dot{u}\\ \dot{v}\\ \dot{w}\end{bmatrix}\end{aligned}\tag{7}$$

The element volume is defined as V_e, then the integration is used to get the force acting on an finite element.

$$\begin{aligned}\vec{F}_g^e &= -\int_{V_e}\rho\vec{\ddot{R}}dV_e\\ &= -\int_{V_e}\rho\begin{bmatrix}\ddot{u}\\ \ddot{v}\\ \ddot{w}\end{bmatrix}dV_e+\Omega^2\int_{V_e}\rho[S]^T[S]\begin{bmatrix}u\\ v\\ w\end{bmatrix}dV_e\\ &\quad+\Omega^2\int_{V_e}\rho[S]^T[S]\begin{bmatrix}x_0\\ y_0\\ z_0\end{bmatrix}dV_e-2\Omega\int_{V_e}\rho[S]\begin{bmatrix}\dot{u}\\ \dot{v}\\ \dot{w}\end{bmatrix}dV_e\end{aligned}\tag{8}$$

in which U can be given by

$$U=\begin{bmatrix}u\\ v\\ w\end{bmatrix}=[N]U^e=[N]\begin{bmatrix}u\\ v\\ w\end{bmatrix}^e\tag{9}$$

where U^e is the node displacement and $[N]$ contains the FEM shape functions. Substituting Eq.(9) into Eq.(8) yields,

$$\begin{aligned}\vec{F}_g^e &= -\int_{V_e}\rho[N]\ddot{U}^e dV_e-2\Omega\int_{V_e}\rho[S][N]\dot{U}^e dV_e\\ &\quad+\Omega^2\int_{V_e}\rho[S]^T[S][N]U^e dV_e\\ &\quad+\Omega^2\int_{V_e}\rho[S]^T[S]r_0 dV_e\end{aligned}\tag{10}$$

The FE node load is defined as $\vec{F^e}$, then the virtual work δW done by $\vec{F^e}$ and $\vec{F}_g^e$ on virtual displacement δU^e can be written as:

$$\begin{aligned}\delta W &= -\delta U^{eT}\int_{V_e}\rho[N]^T[N]\ddot{U}^e dV_e\\ &\quad-2\Omega\delta U^{eT}\int_{V_e}\rho[N]^T[S][N]\dot{U}^e dV_e\\ &\quad+\Omega^2\delta U^{eT}\int_{V_e}\rho[N]^T[S]^T[S][N]U^e dV_e\\ &\quad+\Omega^2\delta U^{eT}\int_{V_e}\rho[N]^T[S]^T[S]r_0 dV_e+\delta U^{eT}\vec{F^e}\\ &= -\delta U^{eT}[M]^e\ddot{U}^e-\delta U^{eT}[M_G]^e\dot{U}^e+\\ &\quad\delta U^{eT}[K_c]^e U^e+\delta U^{eT}\vec{Q}_c^e+\delta U^{eT}\vec{F^e}\end{aligned}\tag{11}$$

where $[M]^e$ is the element mass matrix, $[M_G]^e$ is the element Coriolis matrix, $[K_c]^e$ is the element stiffness matrix, $\vec{Q}_c^e$ is the element Centrifugal force vector. The geometric equation can be expressed as:

$$\varepsilon=[\overline{B}]U^e\tag{12}$$

where $[\overline{B}]$ is the element geometric matrix. Then the virtual strain can be written as:

$$\delta\varepsilon=[\overline{B}]\delta U^e\tag{13}$$

and the virtual strain energy can be obtained:

$$\delta V=\int_{V_e}\delta\varepsilon^T\sigma dV_e=\delta U^{eT}\int_{V_e}[\overline{B}]^T\sigma dV_e\tag{14}$$

Virtual displacement principle can be expressed as:

$$\delta W=\delta V\tag{15}$$

substituting Eq.(11) and Eq.(14) into Eq.(15), the element dynamic equation can be obtained,

$$[M]^e\ddot{U}^e+[M_G]^e\dot{U}^e+[K_c]^e U^e+\int_{V_e}[\overline{B}]^T\sigma dV_e=\vec{Q}_c^e+\vec{F^e}\tag{16}$$

where $[K_0]^e=\int_{V_e}[\overline{B}]^T\sigma dV_e$, then integrate all the elements,the governing equation of motion in dynamic analysis can be expressed as:

$$[M]\ddot{U}(t)+([M_G(\Omega)]+[C])\dot{U}(t)+([K_0]+[K_c(\Omega)])U(t)=F(t)\tag{17}$$

where $[M]$, $[C]$ and $[K_0]$ are mass, damping and stiffness matrices, respectively; $[M_G(\Omega)]$ is the Coriolis matrix,which is a skew symmetric matrix as $[S]$(Eq.(6)) is a skew symmetric matrix; and $[K_c(\Omega)]$ is the centrifugal stiffness matrix.

Finite element model and ANSYS operating method

The finite element model of a realistic compressor bladed disk(Fig.2) with 87,000 degrees-of-freedom(DOFs), contains 24 blades. ANSYS 11.0 is used to establish the FE model and the eight-noded quadratic solid element named SOLID185 is used for modeling. Boundary condition is based on the real assembly relation: axial restraint is imposed on the front surface of the disk center hole, circumferential restraint is imposed on the spline surface, and radial restraint is imposed on the radial bearing mounting surface. The working rotating speed is 11516 rpm. Firstly, Finite element method is used to study the effect of Coriolis force and centrifugal force on the modal characteristics of tuned and mistuned bladed disk; secondly, FEM is used to get the mass matrix, stiffness matrix, and Coriolis matrix, then harmonic response characteristics are simulated by Matlab code.

Fig.3 shows the operating method of ANSYS for calculating the vibration characteristic of bladed disk with Coriolis effect. Firstly, Static analysis is performed to calculate the centrifugal stiffness matrix $[K_c(\Omega)]$, Coriolis matrix $[M_G(\Omega)]$, mass matrix $[M]$ and stiffness matrices $[K_0]$. In this step, APDL commands "CORIOLIS,ON,,,OFF" means activating the Coriolis effect and using the rotating reference frame. Secondly, either Modal analysis or Response analysis can be performed. In modal analysis, APDL commands "MODOPT,QRDAMP,K" means using QR damped method to solve K modes. As This method gives good results for lightly damped systems and can also apply to any arbitrary damping type, it is suitable for solving the structure modal characteristic with Coriolis effect. As the accuracy of this method is dependent on the number of modes K used in the calculations, a sufficient number of fundamental modes should be present to provide good results. This method outputs both the real and imaginary eigenvalues (frequencies), but outputs only the real eigenvectors (mode shapes). In harmonic response analysis, $[M]$, $[K_0]$, $[M_G(\Omega)]$ and $[K_c(\Omega)]$ are extracted from ANSYS, then equations of motion are solved using MATLAB.

Modal characteristics of tuned bladed disk

In this section, the modal characteristics of tuned bladed disk, including the effects of centrifugal force, Coriolis force, and both of the two factors, are presented.

Centrifugal effect

The free vibration characteristics of a tuned bladed disk with the effect of centrifugal force are studied. The rotating speed is from 0 to 1206rad/s. In Fig.4, The natural frequencies of the first eighty modes are plotted. As it can be seen from Fig.4, there are three mode families,namely,1st bending, 2nd bending and 1st torsion. Fig.5 shows the blade mode shape of the first three families. The major conclusions are summarized as follows:

(1) The frequencies of the tuned bladed disk increase with the increase of the rotating speed, which is the result of centrifugal or rotation stiffening effect. As the stiffness of the bladed disk is proportional to the square of rotating speed, rotating speed-frequency curve(Fig.6) is similar to a quadratic curve.

(2) The frequency increment is related to the mode shape of the blade. The frequencies of the first family modes increase by an average of 160Hz, while that of the third family modes increase by an average of only 50Hz. The main cause of this phenomenon is that the direction of the centrifugal force is along the radial direction of the bladed disk, and it can only increase the radial stiffness of the blade.From Fig.5, the first family modes are 1st bending modes of blade which are greatly influenced by the ra-

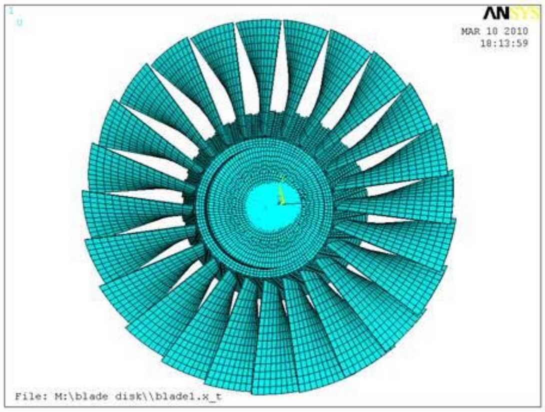

FIGURE 2: Finite element model of a bladed disk

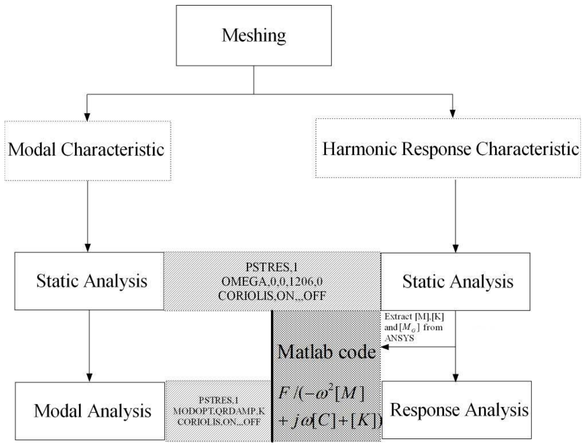

FIGURE 3: ANSYS operating method

dial stiffness, the frequencies of the first family modes will increase obviously with the increase of rotating speed. However, the third family modes are 1st torsion modes of blade which are affected by the torsional stiffness. As the torsional stiffness will not increase with the increase of rotating speed, the frequency will not change obviously.
(3)There is little change in most mode shapes with the increasing of rotating speed. However, some mode shapes are significantly influenced by the centrifugal force, which may change the coupling degree between the blade and the disk. Fig.7 shows the mode shape of 1-nodal diameter modes with different rotating speed. It is found that the coupling degree between the blade and the disk increases with the increase of rotating speed. The strong interaction between the blade and disk will influence Coriolis effects significantly, and it will be presented in the following section.

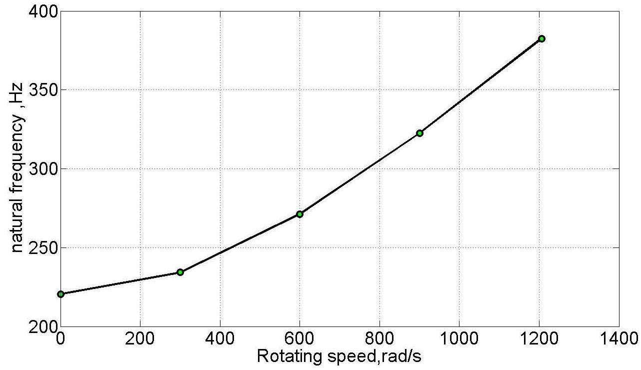

FIGURE 6: Rotating speed - frequency map (1ND Natural frequency of the 1st family)

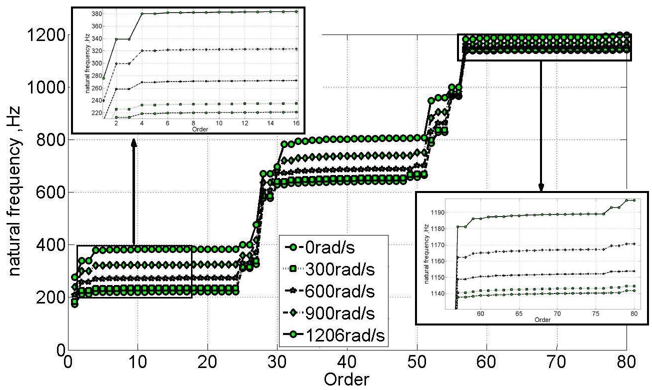

FIGURE 4: The first 80 orders natural frequencies at different rotating speed

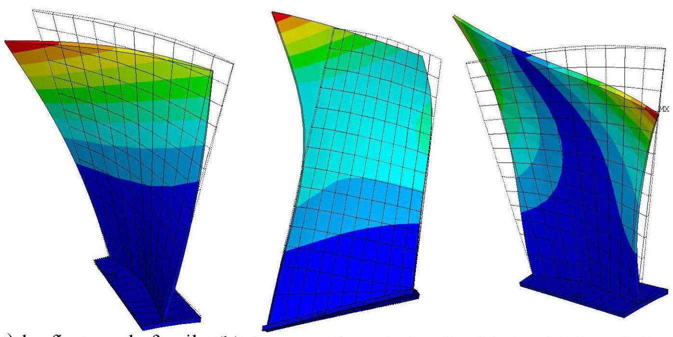

(a)the first mode family: 1st bending (b) the second mode family: 2nd bending (c) the third modefamily: 1st torsion

FIGURE 5: The blade mode shape of the first three families

Coriolis effects

Coriolis effects on the frequencies of the first three families of the bladed disk modes are given in Fig.8. The rotating speed of the bladed disk model is 1206rad/s in this section, and (a) and (b) of these figures represent the Nodal diameter number vs Natural frequency curve and the frequency split curve,respectively. The largest natural frequency splits of first three families of modes are 1.81%, 5.82% and 6.58%, respectively. It can be concluded that:
(1)when Coriolis force are taken into account, those double modes with k nodal diameter (except k=0,12) split into pairs of single modes with different nature frequencies and with mode shapes corresponding to a forward and backward traveling wave mode. A forward traveling wave, defined with respect to the rotating reference frame, is a wave that travels in the same direction as the rotation of the bladed disk, while a backward traveling wave moves in the opposite direction to the bladed disk rotation. Backward traveling wave mode receives more attention in engineering analysis of bladed disk vibration characteristics as the backward traveling modes can be excited by the real aerodynamic excitation.
(2)The largest natural frequency splits of all three mode families are obtained for 1ND(1 nodal diameter) mode, and the frequency split decreases as the nodal diameter number increases. The main cause of this phenomenon is that the coupling level between the blade and the disk is higher with the lower numbers of nodal diameters. With the rise of the coupling level between the blade and the disk, the vibration of the disk will be strengthened. As for the influencing factors of the high vibration level of the disk in the mode of the bladed disk, two main aspects of the Coriolis effect can be divided: one is that the vibration of the disk itself will enhance the effect of Coriolis force; the other reason is that the vibration velocity and direction of blade will be influenced

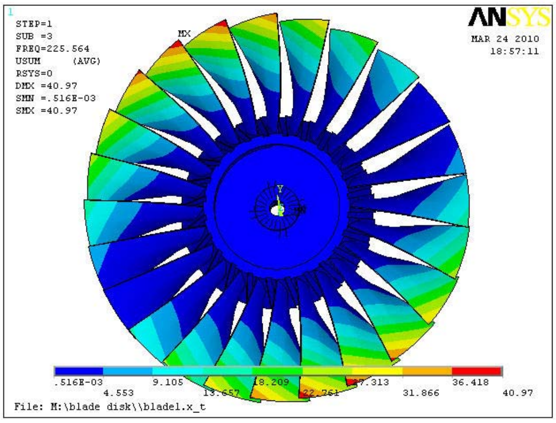

(a) 300 rad/s

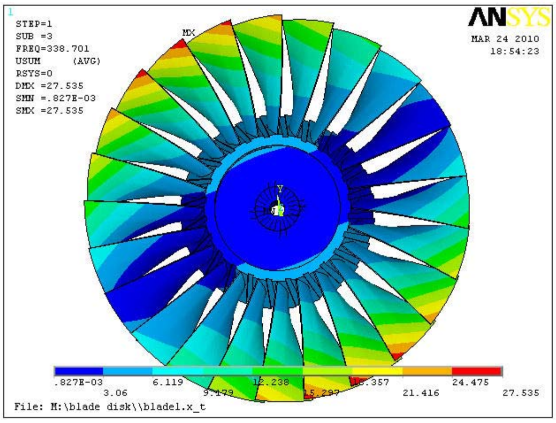

(b) 1206 rad/s

FIGURE 7: 1ND Mode shapes of the 1st family with different rotating speed

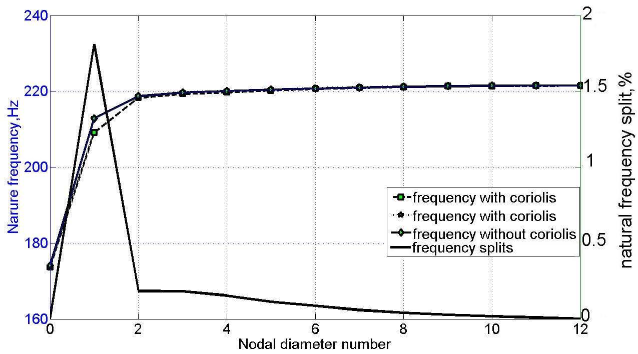

(a) Nature frequencies and frequency splits of the 1st mode family

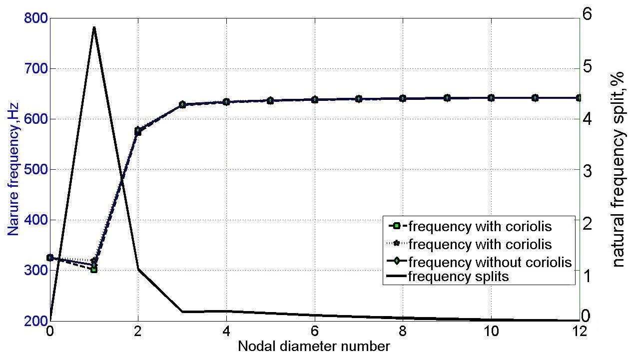

(b) Nature frequencies and frequency splits of the 2nd mode family

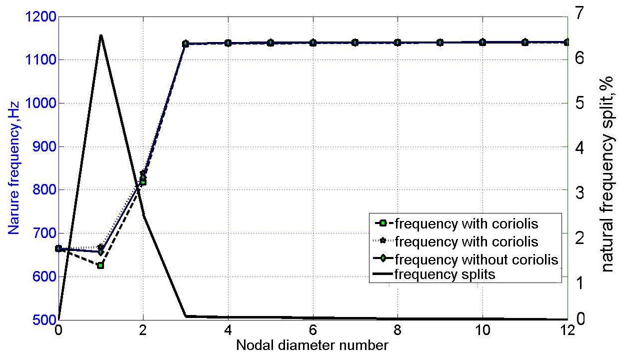

(c) Nature frequencies and frequency splits of the 3rd mode family

FIGURE 8: Nature frequencies and frequency splits

by the vibration velocity and direction of the disk on which the blade is fixed.

(3)Fig.9 shows the 1ND mode shapes of the first two mode families. It can be seen that the disk vibration displacement of the first 1ND mode vibration is lower than that of the second 1ND mode, thus the coupling level between the blade and disk of the first 1ND mode is lower than that of the second 1ND mode. As a result, the effect of Coriolis force on the first 1ND mode is smaller and the corresponding frequency split is smaller. As it can be seen that the coupling levels between the blade and the disk are different with different modes, and they will significantly influence the Coriolis-induced frequency split.

Coriolis effects and centrifugal effect

Fig.10 shows the Nodal diameter number vs Natural frequency curve of the 1st mode family with different rotating speed. There are three curves corresponding to each kind of rotating speed, two of which are the frequency curves with the ef-

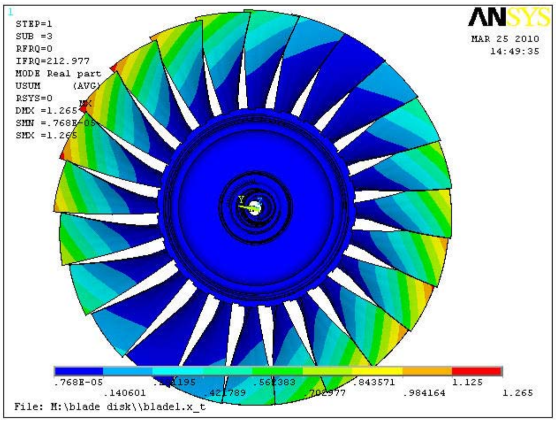

(a) 1ND mode shap of the 1st family

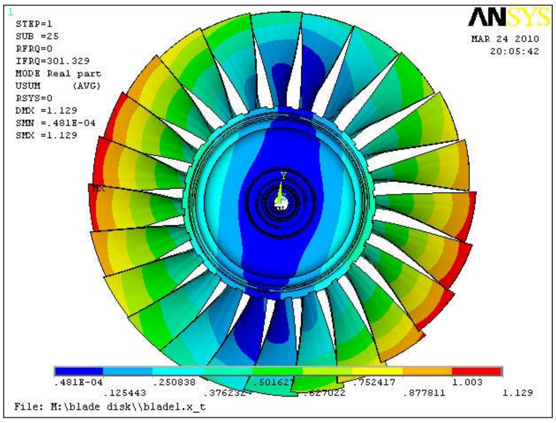

(b) 1ND mode shap of the 2nd family

FIGURE 9: Tuned mode shapes with Coriolis force

fects of Coriolis force and centrifugal force, and the third one is the curve with the effect of centrifugal force only. From Fig.10, the following conclusions can be drawn:

(1) Frequencies of the 1st mode family increase with the increase of the rotating speed, which is the result of centrifugal stiffening effect, and the frequency splits also increase with the increase of the rotating speed(Fig.11), which is the result of the Coriolis effect.

(2) The rotating effect is a coupling interactions between Coriolis force and centrifugal force. The frequency split of the 1ND mode of the 1st family is 3.96Hz for only considering Coriolis effect when the rotating speed is 1206 rad/s. However, it increases to 15.96Hz when considering both Coriolis force and centrifugal force with the same rotating speed. It can be seen from Fig.7 that the stiffness of the blade increases more quickly than that of the disk with the increase of the rotating speed. Furthermore, the stiffness difference of the blade and disk is reduced and the coupling level is increased, which lead to the enhancement of Coriolis effects. Thus the centrifugal force may influence Coriolis effects significantly.

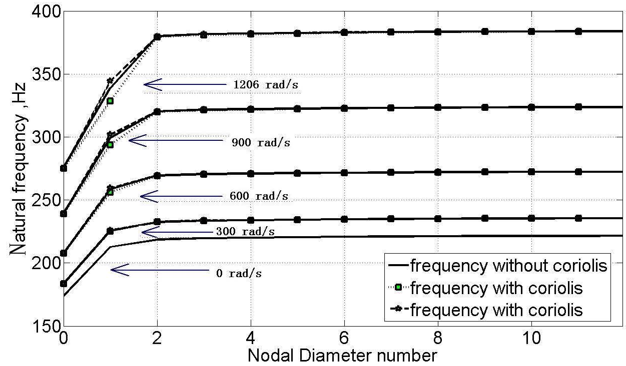

FIGURE 10: Nodal diameter- frequency map of the 1st family with different rotating speed

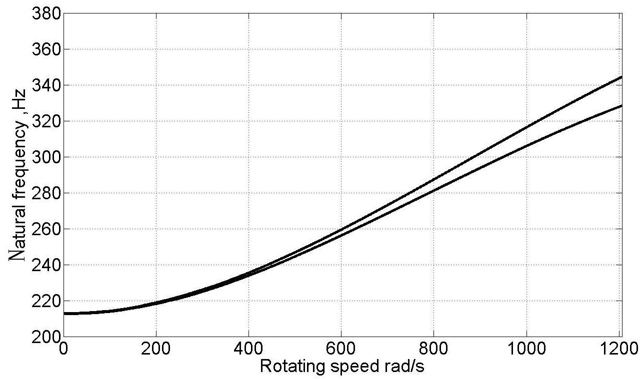

FIGURE 11: Rotating speed - frequency map

Modal characteristics of mistuned bladed disk

In this section, the modal characteristics of mistuned bladed disk, including the effects of centrifugal force, and both of Coriolis force and centrifugal force, are presented. An intentional mistuning pattern (mistuning pattern 1) is shown in Fig.12, which is an elastic module mistuning. The mode analysis is calculated for the mistuned bladed disk.

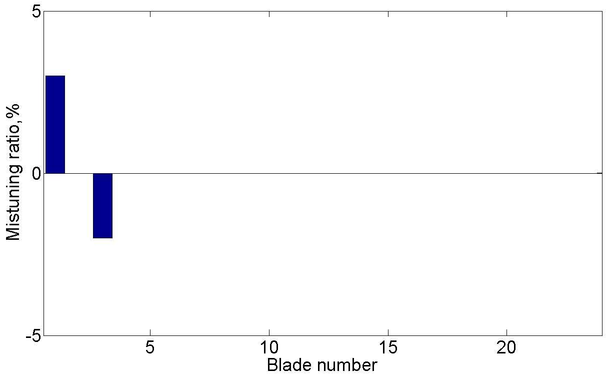

FIGURE 12: Mistuning pattern 1

Definitions of mode localization factor and Coriolis influence factor

Mode localization factor is often used to describe the difference between the mistuned and tuned mode shapes. Wang [17] [18] gave the definition of MLF based on the nondimensional maximal displacement u of the subeigenvector Φ, u is defined as:

$$u = \frac{max[abs(\Phi)]}{sum[abs(\Phi)]} \tag{18}$$

As u gives the ratio of the maximal vibration amplitude and the sum of the vibration amplitudes of all sectors and, it means that the vibration mode will localized in a single sector with the increase of u. For a pair of modes, before and after the mistuning is introduced into the bladed disk, the MLF of a mistuned mode can be defined as:

$$MLF = \frac{u_m - u_n}{u_n} \tag{19}$$

where u_m and u_n are the dimensionless maximal displacements for the mistuned and corresponding tuned mode shape.

To describe the difference between the mode shape of a mistuned bladed disk with and without Coriolis effects, we define the Coriolis impact factor (CIF) as:

$$CIF = \frac{u_C - u_{NC}}{u_{NC}} \tag{20}$$

where u_C and u_{NC} are the dimensionless maximal displacements for the mistuned mode shape with and without Coriolis effects. The difference between the MLF and CIF is that the calculation of MLF needs the dimensionless maximal displacements for both mistuned and tuned mode shape, but the calculation of CIF only need the dimensionless maximal displacements for mistuned mode shape. The value of CIF indicates Coriolis effects on the mode localization of a mode shape. CIF=0 means that Coriolis force has no effect on the mode localization of mistuned bladed disk; $CIF>$ 0 means Coriolis force enhances the localization of that bladed disk.

The definition of CIF have two advantages: First, it is directly connected to the modal displacement and can reflect the effect of Coriolis force on the localization phenomenon directly. Secondly, it is easy to compute and only need the information of the mistuned mode.

Centrifugal effect

The effect of centrifugal force on the modal characteristics of a mistuning(Mistuning pattern 1) bladed disk with different rotating speed is studied, and the value of the calculated MLFs for every mode(1-50) is shown in Fig.13. the MLF value of the 24th and 49th modes are bigger than the other modes. 0 ND and 12ND modes are more sensitive to mistuning, and modal localization of these modes are easier to occur [19].

It can be seen that with increasing rotating speed, a decrease in the MLF of the 24th and 49th modes can be observed. However, there is no obvious rule of the MLFs of the other modes. Therefore, the result shows that the mode localization can be influenced by the centrifugal stiffening effect, but the influence has no distinct rule.

FIGURE 13: Localization factors(MLF) with different rotating speed

Coriolis effects and centrifugal effect

Fig.14 shows the CIFs of 1st to 24th modes with different rotating speed. It can be seen from the figure that the CIFs of all modes are low when the rotating speed is 600rad/s. However, when the rotating speed increases to 900rad/s and 1206rad/s, the CIFs of most modes increase obviously, and the maximum value of all the CIFs is more than 100%. Taking the 7th, 10th, 18th and 19th modes as an example, Coriolis force has no effect on the localization of these mode shapes when the rotating speed is 600rad/s, while it influences the localization of the four mode shapes significantly when the rotating speed is up to 1206rad/s. For the 6th mode, Coriolis force has an opposite effect and the CIF is a negative value, that means Coriolis force can demonstrate a substantial reduction in the mode localization phenomenon. Fig.15 and Fig.16 which are the mode shapes of the 7th and 6th modes can demonstrate the correctness of above analysis.CIF value of the 7th mode is greater than 100% when the rotating speed is 1206rad/s, which means the coriolis effect enhances the localization of this mode. It can be seen from Fig.15 that the localization phenomenon of (b)(with Coriolis effect) is stronger than (a)(without Coriolis effect). CIF value of the 6th mode is less than 0 when the rotating speed is 1206rad/s, which means the coriolis effect reduces the localization of this mode. It can be seen from Fig.16 that the localization phenomenon of (a)(without Coriolis effect) is stronger than (b)(with Coriolis effect).

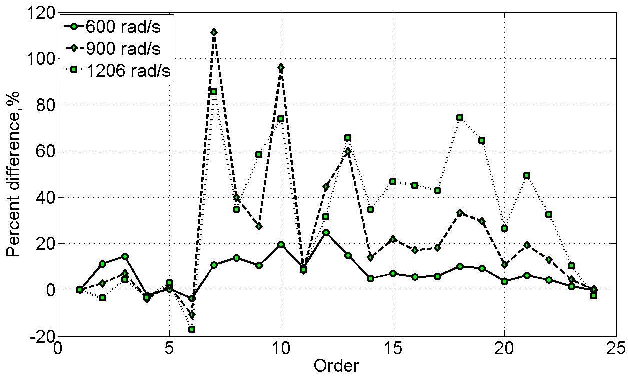

FIGURE 14: Coriolis impact factors(CIF) with different rotating speed

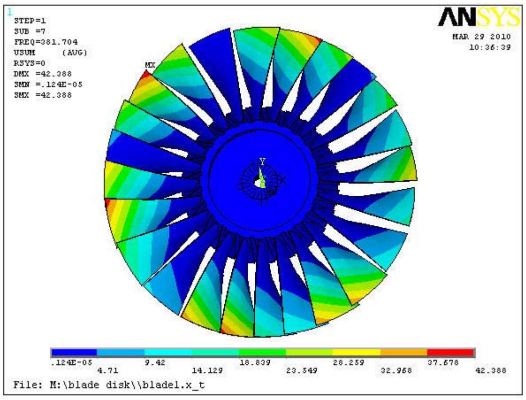

(a) without Coriolis force

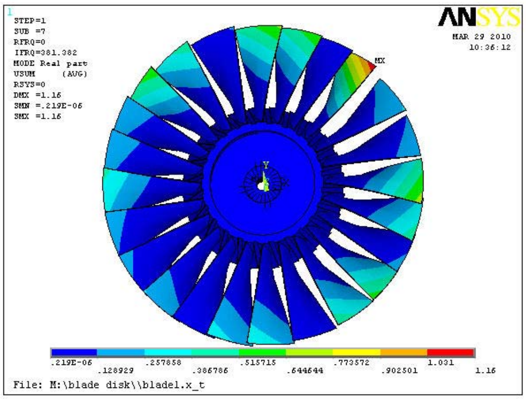

(b) with Coriolis force

FIGURE 15: The 7th order mistuned modal shapes

Forced response analysis of tuned bladed disk

The structural damping is specified through critical damping ratio ξ, which is about 0.1% in the response analysis of bladed disk structure [20], so the constant mass matrix multiplier α is set to 2.094 and the constant stiffness matrix multiplier β is set to 2.653e-3 in this study. Then the harmonic response characteristic of tuned bladed disk is studied in this section, including Coriolis effects and centrifugal force. The vibration responses to an engine order excitation with EO=1 and an excitation amplitude of F=1N are shown in Fig.17 (with Coriolis force) and Fig.18(with Coriolis force and centrifugal force). From the two figures, the following conclusions can be drawn:

(1) When the bladed disk is tuned, the response amplitudes of each blade is the same.

(2) The effect of centrifugal force is divided into two aspects: one is that it can increase the resonance frequency of the bladed disk, the other is it can decrease the resonance amplitude.

(3) There are one backward(EO=+1) traveling wave and one forward(EO=-1) traveling wave forced responses of tuned bladed disk. In the case of a tuned system without Coriolis force, the backward and forward traveling wave responses are identical, whereas the presence of Coriolis forces generates these forced responses at distinct frequencies.

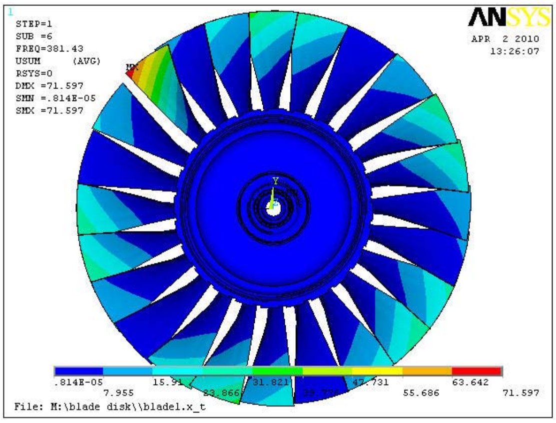

(a) without Coriolis force

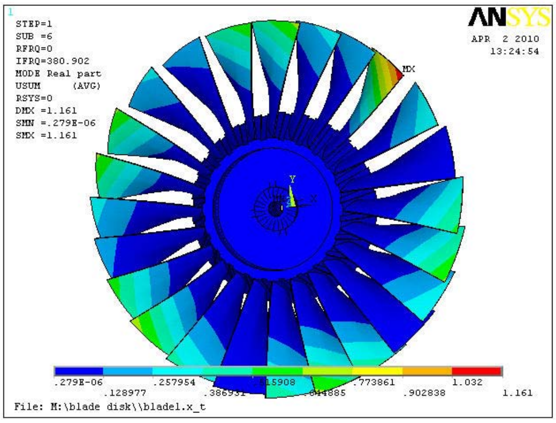

(b) with Coriolis force

FIGURE 16: The 6th order mistuned modal shapes

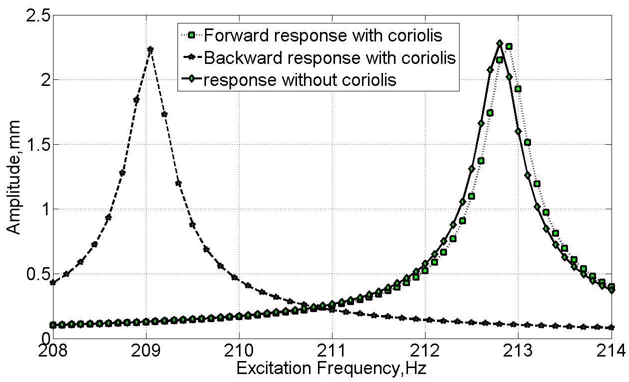

FIGURE 17: Tuned forced responses without Centrifugal force

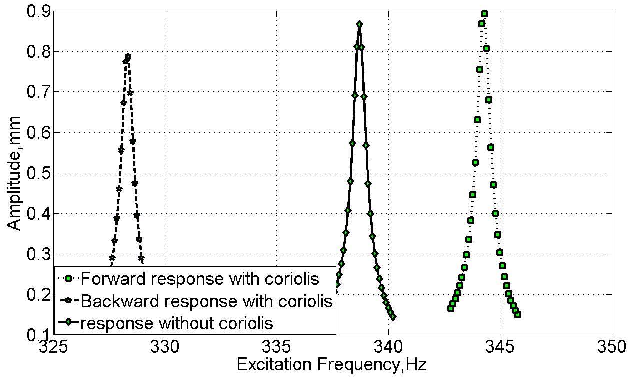

FIGURE 18: Tuned forced responses with Centrifugal force

TABLE 1: Maximum amplitudes of the bladed disk, Mistuning pattern 1(mm)

Excitation engine order	A(Without Coriolis force)	B(With Coriolis force)	B-A (%)
1	0.9188	0.8967	-2.4053
2	0.8034	0.8050	0.1992
3	0.8812	0.9337	5.9578
4	0.7738	0.7883	1.8739
5	0.9013	0.7783	-13.6470
6	0.9222	0.9130	-0.9976
12	0.7839	0.6131	-21.7885

Forced response analysis of mistuned bladed disk

In this section, harmonic response characteristic of mistuned bladed disk with Coriolis effect and centrifugal effect is studied. There are three kinds of mistuning patterns: mistuning pattern 1 in section 3.3 and two random mistuning patterns with a mistuning strength of [-1%,1%], which is depicted in Fig.19. Harmonic response characteristics of the bladed disk with three kinds of mistuning pattern are investigated, and the traveling wave excitations with EO from 1 to 6 and 12 are taken into account.

Fig.20, Fig.21 and Fig.22 show the maximum response amplitudes of all blades under ±3EO, ±6EO and ±2EO traveling excitation, respectively. As can be seen from Fig.20 that the maximum response amplitude of bladed disk with mistuning pattern

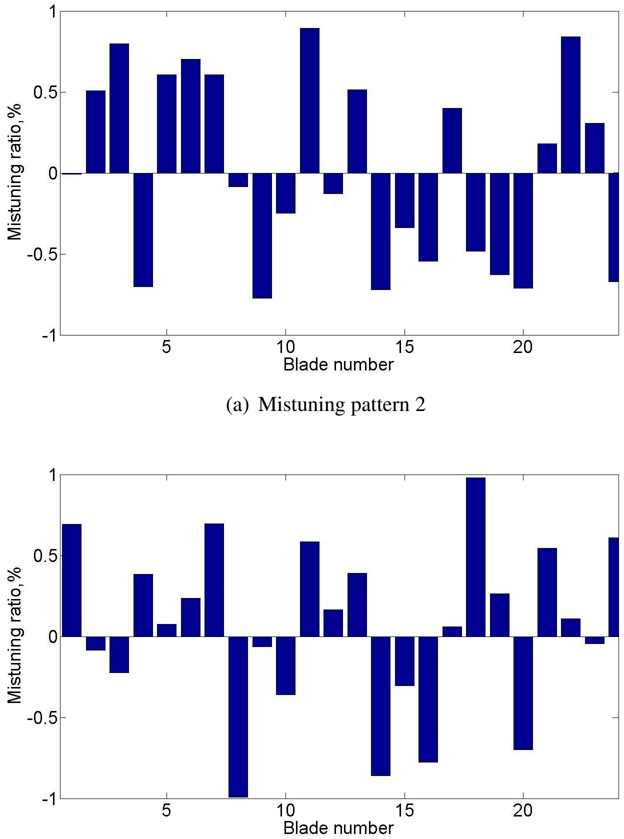

(a) Mistuning pattern 2

(b) Mistuning pattern 3

FIGURE 19: Random mistuning patterns

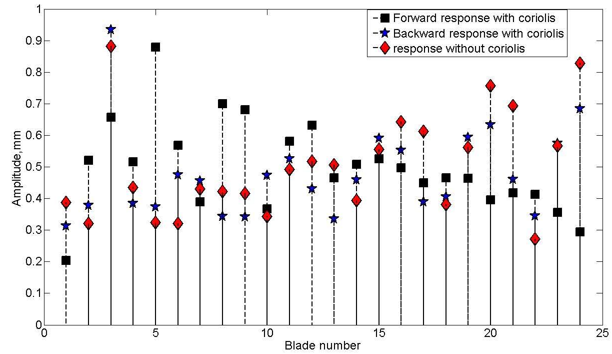

FIGURE 20: Maximum blade amplitudes(±3EO),mistuning pattern 1

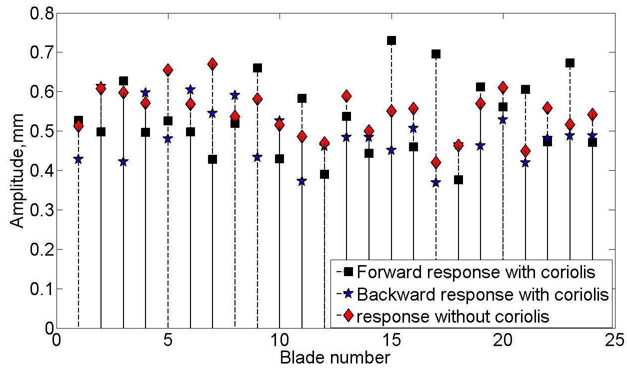

FIGURE 21: Maximum blade amplitudes(±6EO),mistuning pattern 2

1 under ±3EO traveling excitation increases 5.96% when considering Coriolis effect. In contrast to this, the maximum response amplitude of bladed disk with mistuning pattern 2, under ±6EO traveling excitation increases 8.85%(Fig.21), and the maximum response amplitude of bladed disk with mistuning pattern 3, under ±2EO traveling excitation decreases -16.50%(Fig.22). Table 1, Table 2 and Table 3 show the maximum response amplitudes of bladed disk with and without Coriolis effect. Different mistuning patterns and different excitation engine orders are also considered in these tables. The following conclusions can be drawn:
(1) Coriolis force affects the response characteristics of the mistuned bladed disk significantly, and the influencing Effect of Coriolis force is related to the mistuning pattern and excitation engine order(Table 1 -Table 3).
(2) The amplitude spread as a function of blade number, depicted in Fig.20, Fig.21 and Fig.22, shows that Coriolis force not only influences the maximum amplitude of the bladed disk, but all the maximum blade amplitudes as well.
(3) The backward traveling excitation by +12EO is coincident with the forward traveling excitation by -12EO, so the corresponding backward and forward responses are identical. However, the backward and forward responses excited by the other engine orders are different.
(4) Centrifugal force could decrease the response amplitude of the blades disk and reduce the difference of different maximum blade amplitude.

Conclusions

Coriolis effects and centrifugal effect on the vibration behavior of tuned and mistuned realistic bladed disk are investigated in this paper for the first time, The major conclusions that can be drawn from this study, are given as:
(1) Double modes with k nodal diameter (except k=0,12) split into pairs of single modes(two different nature frequencies) with Coriolis effects. The largest natural frequency split of one mode family are obtained for 1ND mode, and the frequency split decreases as the nodal diameter number increases. The largest natural frequency splits between different mode families are quite

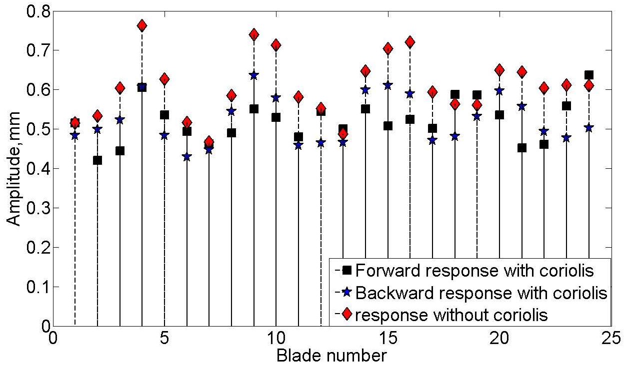

FIGURE 22: Maximum blade amplitudes(±2EO),mistuning pattern 3

TABLE 2: Maximum amplitudes of the bladed disk, Mistuning pattern 2(mm)

Excitation engine order	A(Without Coriolis force)	B(With Coriolis force)	B-A (%)
1	0.8799	0.8864	0.7387
2	0.7699	0.6622	-13.9888
3	0.6994	0.7377	5.4761
4	0.7284	0.7490	2.8281
5	0.6730	0.6033	-10.3566
6	0.6704	0.7297	8.8455
12	0.7689	0.7556	-1.7297

different, and the value is related to the mode shape.
(2) Coriolis force influences the localization of the mode shapes significantly. The mode localization phenomena of some modes are increased, others are reduced.
(3) Coriolis force affects the response characteristics of the mistuned bladed disk significantly, and the influencing effect of Coriolis force is related to the mistuning pattern and excitation engine order.
(4) Centrifugal force can change the coupling degree between the blade and the disk, which will influence Coriolis effect.

TABLE 3: Maximum amplitudes of the bladed disk, Mistuning pattern 3(mm)

Excitation engine order	A(Without Coriolis force)	B(With Coriolis force)	B-A (%)
1	0.8803	0.8875	0.8179
2	0.7623	0.6365	-16.5027
3	0.6805	0.6629	-2.5863
4	0.6862	0.6805	-0.8307
5	0.7210	0.6198	-14.0361
6	0.6977	0.7215	3.4112
12	0.7537	0.7470	-0.8889

ACKNOWLEDGMENT

This work has been supported by the National High Technology Research and Development Program of China under grant 2008AA-042403.

REFERENCES

[1] Wang, J.J. and Li, Q.H., 2009, “Vibration and applications of reduction modeling for mistuned bladed disk in aero-engine,” National Defense Industry Press, Beijing
[2] Ewins, D. J., 1976, “Vibration modes of mistuned bladed disks,” ASME Journal of Engineering for Gas Turbines and Power, 98(3), pp349-355
[3] Sinha, A., 2007, “Reduced-Order model of a bladed rotor with geometric mistuning,” Proceedings of ASME Turbo Expo 2007, Montreal, Canada, GT2007-27276
[4] Petrov, E.P., 2010, “Reduction of forced response levels for bladed discs by mistuning overview of the phenomenon,” Proceedings of ASME Turbo Expo 2010, Glasgow, UK, GT2010-23299
[5] Ersin, Y. M. ., Ender, C. and Nevzat, O. H., 2010, “Nonlinear forced response analysis of mistuned bladed disk assemblies,” Proceedings of ASME Turbo Expo 2010, Glasgow, UK, GT2010-22128
[6] Wang, J.J., Li, Q. H. and Zhu, Z.G., 2000, “Vibration localization of mistuned bladed disk assemblies: A review,” Advances in Mechanics, 30(4), pp517-528
[7] Castanier, M. P. and Pierre, C., 2006, “Modeling and Analysis of Mistuned Bladed Disk Vibration: Status and Emerging Directions,” Journal of Propulsion and Power, 22(2), pp384-

396
[8] Leissa, A W., Lee,J K. and Wang, A J., 1981, “Rotating blade vibration analysis using shells,” American Society of Mechanical Engineers,9-12
[9] Xu, Z. l., Li, X. Y., Park, J. P. and Ryu, S. J., 2003, “Effect of Coriolis acceleration on dynamic characteristics of high speed spinning steam turbine blades,” Journal of Xi’an Jiaotong University, 37(9), pp894-897
[10] Ewins. D.J., 2000, “Modal Testing: Theory, Practice and Application,” Second Edition, Research Studies Press
[11] Sakata. M., Kimura. K. and Park, S.K., 1989, “Vibration of blade flexible rotor due to gyroscopic moment,” Journal of Sound and Vibration, 131(3), pp417-430
[12] Jacquet, G., Ferraris, G. and Rieutord, P., 1996, “Frequencies and modes of rotating flexible bladed disc-shaft assemblies: a global cyclic symmetry approach,” Journal of Sound and Vibration, 191(5), pp901-915
[13] Chun, S.B. and Lee, C.B., 1996, “Vibration analysis of shaft-bladed disk system by using substructure synthesis and assumed modes method,” Journal of Sound and Vibration, 189(5):587-608
[14] Khader, N. and Masoud, S., 1991, “Vibration of mistuned blade disks supported by flexible continuous shafts,” Journal of Sound and Vibration, 149(3), pp471-488
[15] Nikolic, M., Petrov, E.P. and Ewins, D.J., 2007, “Coriolis forces in forced response analysis of mistuned bladed disks,” Journal of Turbomachinery, 129(4), pp730-739
[16] Huang, B. W. and Kuang, J. H., 2001, “Model localization in a rotating mistuned turbo disk with coriolis effect,” International Journal of Mechanical Sciences, 43, pp1643-1660
[17] Wang,J.J., Yao,J.Y. and Li,Q.H., 2008, “Probability characteristics of vibratory mode of bladed disk assemblies with random stiffness mistuning,” Journal of aerospace Power, 23(2), pp256-262
[18] Wang,J.J., Yu,C.B., Yao, J.Y., and Li, Q.H., 2009, “Vibratory mode localization factors of mistuned bladed disk assemblies,” Journal of propulsion technology, 30(4), pp457-461
[19] Yu,C.B., 2010, “Investigation on the Modeling Method and Vibratory Characteristics of Mistuned Blades Disk Structures,” Ph.D. Dissertation, Beijing University of Aeronautics and Astronautics
[20] Seinturier. E. and Lombard, J.P., 2004, “Forced response prediction methodology for the design of HP compressors bladed disks,” Proceedings of ASME Turbo Expo 2004, Vienna, Austria, GT-2004-53372

